Synthesis, Characterization, and Thermodynamic Properties of the Rare Earth Coordination Complex [Sm(C6H4NO2)2·C9H6NO]

ARTICLE *in* INDUSTRIAL & ENGINEERING CHEMISTRY RESEARCH · MARCH 2012

Impact Factor: 2.59 · DOI: 10.1021/ie202891s

7 AUTHORS, INCLUDING:

Hui-Wen Gu
Hunan University
33 PUBLICATIONS **102** CITATIONS

SEE PROFILE

I&EC research
Industrial & Engineering Chemistry Research

Article

pubs.acs.org/IECR

Synthesis, Characterization, and Thermodynamic Properties of the Rare Earth Coordination Complex $[Sm(C_6H_4NO_2)_2{\cdot}C_9H_6NO]$

Hui-Wen Gu,[†,‡] Sheng-Xiong Xiao,*[,‡] Hang-Ying Xiao,[‡] Yun Xiao,[§] Ai-Tao Li,[‡] Xiao-Li Hu,[‡] and Qiang-Guo Li[‡]

[†]State Key Laboratory of Chemo/Biosensing & Chemometrics, College of Chemistry and Chemical Engineering, Hunan University, Changsha 410082, Hunan Province, P.R. China

[‡]Hunan Provincial Key Laboratory of Xiangnan Rare-Precious Metals Compounds and Applications, Department of Chemistry and Life Science, Xiangnan University, Chenzhou 423000, Hunan Province, P.R. China

[§]Key Laboratory of Analysis and Detection Technology for Food Safety of Ministry of Education, College of Chemistry and Chemical Engineering, Fuzhou University, Fuzhou 350002, Fujian Province, P.R. China

Supporting Information

ABSTRACT: This article reports the synthesis and thermodynamic properties of a novel rare earth coordination complex, samarium chloride hexahydrate ($SmCl_3{\cdot}6H_2O$) with nicotinic acid ($C_6H_5NO_2$) and 8-hydroxylquinoline (C_9H_7NO), whose composition and structure were characterized by elemental analysis, molar conductance, thermogravimetric analysis (TG−DTG), UV spectroscopy, IR spectroscopy, and X-ray powder diffraction. During the process of coordination, $C_6H_5NO_2$ was bidentate-coordinated with the rare earth ion (Sm^{3+}) through an acidic group that was formed by removing the proton; the hydroxyl oxygen atom and heterocyclic nitrogen atom of $C_9H_6NO^-$ formed a chelate ring with Sm^{3+} for coordination. The X-ray powder diffraction pattern demonstrated that the crystal type of $[Sm(C_6H_4NO_2)_2{\cdot}C_9H_6NO]$ is similar to that of $C_5H_{11}NO_2$, with the cell parameters a = 5.426 nm, b = 22.105 nm, and c = 5.277 nm. At a constant temperature of 298.15 K, the dissolution enthalpies of the reactants and products of the coordination reaction in the optimized calorimetric solvent were determined with an advanced solution−reaction isoperibol microcalorimeter. The standard molar enthalpy change of the coordination reaction was determined to be $\Delta_r H_m^{\Theta}$ = (167.49 ± 0.39) kJ·mol^{-1}. The standard molar enthalpy of formation of the title complex, $[Sm(C_6H_4NO_2)_2{\cdot}C_9H_6NO]$, was estimated to be $\Delta_f H_m^{\Theta}[Sm(C_6H_4NO_2)_2{\cdot}C_9H_6NO(s), 298.15\ K]$ = −(1483.4 ± 2.4) kJ·mol^{-1}, from a combination of the experimental values of enthalpies of dissolution and some other auxiliary thermodynamic data through a designed thermochemical cycle based on a supposed chemical reaction.

1. INTRODUCTION

Rare earth ions are known to exhibit antibacterial, antitumor, and antivirus properties when coordinated with organic small-molecule ligands.[1,2] Because of their strong affinity to many biological molecules, rare earth ions can effectively participate in many important life processes and activate or inhibit a variety of enzymes or pro-enzymes. More recent research has shown that nicotinic acid has obvious effects on dilating vessels, decreasing blood lipid, inhibiting synthesis of cholesterol, dissolving fibrin, and restraining the formation of thrombus.[3] Interestingly, complexing ligands such as 8-hydroxylquinoline and its derivatives have also been found to have potential bioactivities, including anticancer, antibacterial, and antioxidative properties; vasorelaxing properties; and antivirus and antiplatelet activities.[4−6] Moreover, the bioactivities of the products from the reaction of rare earth chloride with nicotinic acid or 8-hydroxyquinoline are significantly stronger than those of rare earth ions, nicotinic acid, or 8-hydroxyquinoline alone.[7,8] Thus, the synergetic effects of rare earths with nicotinic acid and 8-hydroxyquinoline in inhibiting the growth of bacteria have attracted increasing attention. Information about the role of rare earth complexes in biological systems, their presence and concentration in different equilibrium are of increasing importance.

Accordingly, in recent years, rare earth coordination complexes have been widely and deeply researched by many scholars all over the world, especially in China. For example, Zhang et al.[9,10] synthesized a series of ternary rare earth coordination complexes and studied their compositions, crystal structures, thermal decomposition behaviors, and nonisothermal kinetics. Also, Li et al.[11,12] investigated their inhibiting effects on the growth of various bacteria and tumor cells. It is well-known that data on standard molar enthalpies of formation play a very important role in the theoretical study, application development, and industrial production of a compound as a basis of theoretical analysis. Standard molar enthalpies of formation, together with standard molar entropies, are equally important data in determining any chemical equilibria.[13] Consequently, research on the thermokinetic and biological properties of rare earth coordination complexes is quite active. However, few studies have been devoted to the standard molar enthalpies of formation of rare earth coordination complexes, especially in the situation that the fundamental thermodynamic

Received: December 9, 2011
Revised: March 5, 2012
Accepted: March 10, 2012
Published: March 10, 2012

dx.doi.org/10.1021/ie202891s | Ind. Eng. Chem. Res. 2012, 51, 4797−4803

database of rare earth coordination complexes is still not sufficient.

Solution−reaction calorimetry is a broad and versatile technique that has the advantages of being rapid, accurate, economical, and convenient. It is now widely applied for the measurements of enthalpies of reaction, dissolution, dilution, mixing, adsorption, and formation, as well as excess enthalpies.[14−16] To further study the thermodynamic properties of rare earth coordination complexes, in this article, we report the synthesis and characterization of the novel rare earth coordination complex $[Sm(C_6H_4NO_2)_2 \cdot C_9H_6NO]$. In particular, its thermodynamic properties were investigated using an advanced solution−reaction isoperibol microcalorimeter,[17] which dramatically improved the accuracy of the dissolution enthalpies of samples, with an accuracy of 99.5%. Obviously, such measurements are indispensable for strict modern experimental technology. We believe that this type of study could benefit the research and development of rare earth coordination complexes.

2. THEORY

According to Hess's law, the standard molar enthalpy change of a chemical reaction can be deduced from the dissolution enthalpies, which can be measured when the reactants and products are dissolved in an optimal calorimetric solvent

$$\Delta_r H_m^\Theta = -\sum_B \nu_B \Delta_s H_{m,T,B}^\Theta \quad (a)$$

The standard molar enthalpy change can also be calculated from the standard molar enthalpies of formation of the relevant reactants and products in a chemical reaction

$$\Delta_r H_m^\Theta = \sum_B \nu_B \Delta_f H_{m,T,B}^\Theta \quad (b)$$

In these two equations, $\Delta_r H_m^\Theta$ represents the standard molar enthalpy change of a chemical reaction; $\Delta_s H_{m,T,B}^\Theta$ represents the dissolution enthalpy of a substance B when it is dissolved in the optimal calorimetric solvent at temperature T; $\Delta_f H_{m,T,B}^\Theta$ denotes the standard molar enthalpy of formation of a substance B at temperature T; and ν_B is the stoichiometric coefficient of the corresponding substance B in a chemical reaction equation, which is negative for reactants and positive for products.

3. EXPERIMENTAL DETAILS

3.1. Chemicals and Reagents. All chemicals and reagents used were of analytical grade; their purities, sources, and purification methods are provided in Table SI-1 (see Supporting Information).

3.2. Methods. FTIR spectra (4000−400 cm^{-1}) were measured on a Fourier transform IR spectrometer (Avatar360, Nicolet, Madison, WI, with a KBr pellet). Ultraviolet spectra were recorded on a UV−visible spectrophotometer (U-3010, Hitachi, Tokyo, Japan). Measurement of thermogravimetry−differential thermal gravimetry (TG−DTG) curves was performed on a thermogravimetry analysis instrument (STA449C, NETZSCH Corporation, Selb, Germany). An elemental analyzer (Perkin-Elmer 2400 CHN, Wellesley, MA) was used to determine the C, H, and N contents of the complex. A digital Abbe refractometer (WAY-IS, Shanghai Precision & Scientific Instrument Co., Ltd., Shanghai, China) was used to measure the molar conductivity of the complex. X-ray powder diffraction patterns were recorded on a D8 advance X-ray powder diffractometer (Bruker Corporation, Ettlingen, Germany) scanning from 5° to 80° using Cu Kα (λ = 1.54187 Å) radiation. The tube voltage was 40 kV, the tube current was 40 mA, the scanning speed was 0.5 s, and the scanning step was 0.02°.

The dissolution enthalpies were measured with an SRC-100 solution−reaction isoperibol microcalorimeter (Figure SI-1, Supporting Information; constructed by the Thermochemical Laboratory of Wuhan University, Wuhan, China).[17] In the calorimetric experiments, the temperature was 298.15 K, the current was 11.760 mA, and the resistance of the heater was 1251.5 Ω. The calibration of the calorimeter was carried out by measuring the dissolution enthalpies of KCl (calorimetric primary standard) in triply distilled water and tris(hydroxymethyl)aminomethane (THAM, NBS 742a) in 0.0001 mol·cm^{-3} HCl at 298.15 K. The mean dissolution enthalpies were (17597 ± 17) J·mol^{-1} for KCl and −(29776 ± 16) J·mol^{-1} for THAM, in agreement with published data [(17536 ± 9) J·mol^{-1} for KCl[17] and −(29766 ± 31.5) J·mol^{-1} for THAM[18]]. The eventual errors of the experimental results were within ±0.5% compared with the recommended reference data, which suggests that the microcalorimeter was feasible.

3.3. Synthesis and Characterization of the Title Complex. Quantitative NaOH/ethanol solution was added to $C_6H_5NO_2$/ethanol solution under slight heating. Then, the sodium salt solution (formed in the preceding procedure) and C_9H_7NO/ethanol solution were mixed. At a constant temperature of 60 °C, samarium chloride/ethanol solution was added dropwise to the mixture. Then, the reaction solution was stirred for 6 h (the pH was adjusted to 6.5−7.0). After overnight deposition and air pump filtration, a solid complex was obtained. The product was washed alternately with ethanol and water at a temperature of 80 °C until no Cl^- was detected in the filtrate. After that, the product was dried in a vacuum desiccator at 60 °C until its mass remained constant. Subsequently, the contents of C, H, and N were determined by individual elemental analyses. The content of Sm^{3+} was determined by ethylenediaminetetraacetic acid (EDTA) titration after the complex had been decomposed by heating with concentrated hydrochloric acid, and the content of crystal water was determined by thermogravimetry−differential thermal gravimetry (TG−DTG). The analytical results showed that the composition of the complex was $[Sm(C_6H_4NO_2)_2 \cdot C_9H_6NO]$, and its purity was more than 99.0%.

3.4. Determination of Dissolution Enthalpies. *3.4.1. Thermochemical Cycle of the Coordination Reaction.* Although the thermal effect of the solid-state coordination reaction was difficult to determine, it was feasible to deduce the enthalpies of formation from the dissolution enthalpies measured when the samples were dissolved in the calorimetric solvent. In this work, a convincing thermochemical cycle based on Hess's law was designed, as shown in Figure 1.

In Figure 1, $C_6H_5NO_2$ denotes nicotinic acid, and C_9H_7NO stands for 8-hydroxylquinoline. The equation of the coordination reaction is as follows

$$SmCl_3 \cdot 6H_2O(s) + 2C_6H_5NO_2(s) + C_9H_7NO(s) \rightarrow [Sm(C_6H_4NO_2)_2 \cdot C_9H_6NO](s) + 3HCl(g) + 6H_2O(1)$$

The UV spectra and refractive indexes of the final solution of the reactants and the final solution of the products can be used to determine whether they have the same thermodynamic state. In the present experiments, we determined the UV spectra and refractive indexes of solutions C and F in Figure 1. The experimental results suggested that the two solutions have similar UV

dx.doi.org/10.1021/ie202891s | Ind. Eng. Chem. Res. 2012, 51, 4797−4803

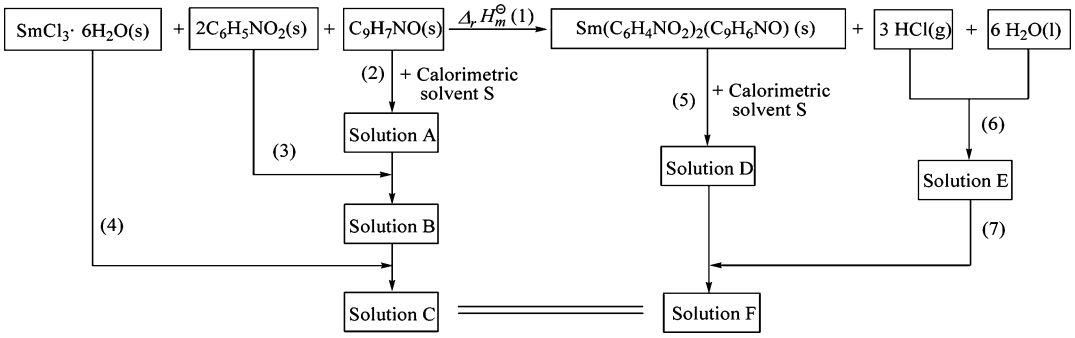

Figure 1. Thermochemical cycle of the coordination reaction.

Table 1. Dissolution Enthalpies [$\Delta_s H_m^{\ominus}$ (kJ·mol^{-1})] of $2C_6H_5NO_2(s)$, $C_9H_7NO(s)$, $SmCl_3{\cdot}6H_2O(s)$, $[Sm(C_6H_4NO_2)_2{\cdot}C_9H_6NO](s)$, and Solution E in the Calorimetric Solvent S at 298.15 K

sample	$2C_6H_5NO_2(s)$	$C_9H_7NO(s)$	$SmCl_3{\cdot}6H_2O(s)$	$[Sm(C_6H_4NO_2)_2{\cdot}C_9H_6NO](s)$	solution E
1	35.019	−2.716	−33.309	−106.633	−11.770
2	35.023	−2.630	−33.669	−106.136	−11.989
3	35.489	−2.644	−33.752	−106.468	−12.027
4	35.006	−2.675	−33.570	−106.418	−11.938
5	35.195	−2.770	−33.736	−106.108	−12.154
average	35.146 ± 0.207	−2.687 ± 0.057	−33.607 ± 0.182	−106.353 ± 0.225	−11.975 ± 0.140

spectra and equal refractive indexes, which demonstrates that they have the same thermodynamic state and that the thermochemical cycle of the designed coordination reaction was reliable.

3.4.2. Choice of Calorimetric Solvent. It is very important to choose a solvent that can dissolve all of the reactants and products rapidly and completely. Research indicated that the relevant substances in the coordination reaction are highly soluble in the mixed solvent of 2 mol·L^{-1} HCl, dimethylformamide (DMF), and ethanol (EtOH). By mixing these three solvents uniformly at different ratios and continually testing the solubility of the samples, the best solubility was found when the volume ratio of the three solvents was $V_{HCl}/V_{DMF}/V_{EtOH}$ = 3:1:1. Consequently, this mixture was chosen as the optimal calorimetric solvent S.

3.4.3. Determination of Dissolution Enthalpies of Reactants and Products. Thoroughly dried samples were ground completely in an agate mortar, and then exactly 0.25 mmol of sample was placed in the sample container of the microcalorimeter. The calorimetric solvent S (100.00 mL) had been added to the reaction vessel in advance. When the calorimeter was adjusted to a constant temperature of (298.150 ± 0.001) K, the samples were added to the reaction vessel, and then their dissolution enthalpies were measured. The results are listed in Table 1 based on five parallel measurements.

4. RESULTS AND DISCUSSION

4.1. Elemental Analysis and General Properties of the Complex. The theoretical values for the elemental analysis of $[Sm(C_6H_4NO_2)_2{\cdot}C_9H_6NO]$ are as follows: C, 46.82%; H, 2.62%; N, 7.80%; Sm, 27.91%. The following values were found: C, 47.12%; H, 2.54%; N, 7.91%; Sm, 27.45%.

The complex was obtained as a yellow powder that was very stable in the atmosphere. It was found to be soluble in dimethylsulfoxide but could not be dissolved in water, chloroform, methanol, ethanol, dimethylformamide, acetone, petroleum ether, and tetrahydrofuran. The molar conductance of the complex in dimethylsulfoxide (DMSO) was determined to be 9.84 S·cm^2·mol^{-1}, indicating that the complex is a nonelectrolyte and exists as a neutral molecule in DMSO.

4.2. Mechanism of Thermal Decomposition. TG−DTG curves of $[Sm(C_6H_4NO_2)_2{\cdot}C_9H_6NO]$ at a heating rate of β = 10 °C·min^{-1} in flowing N_2 are shown in Figure 2. No obvious

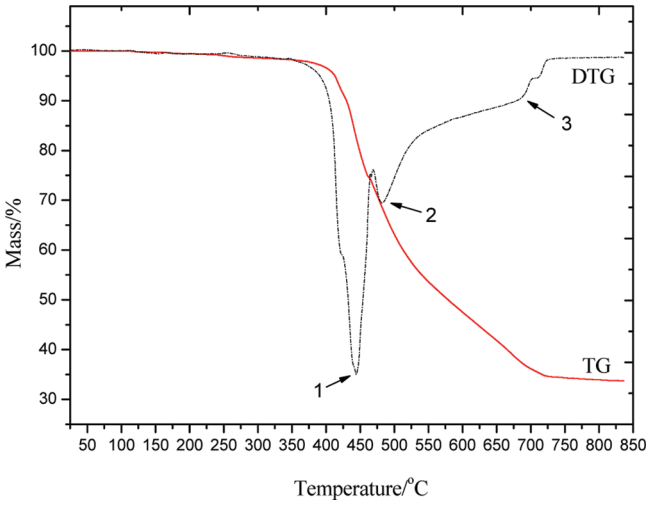

Figure 2. TG−DTG curves (β = 10 °C·min^{-1}) of the complex $[Sm(C_6H_4NO_2)_2{\cdot}C_9H_6NO]$.

mass loss occurred within 200 °C, which indicates that no crystal water exists in the molecular of the complex. The thermal decomposition process can be divided into three steps. The first decomposition process occurs from 387.34 to 465.08 °C with a mass loss of 25.76% corresponding to the loss of 1 mol of $C_9H_6NO^-$ (theoretical loss of 25.27%). The second stage ranges from 465.08 to 548.80 °C with a mass loss of 20.45%, which corresponds to the loss of 1 mol of $(C_6H_4NO_2)^-$ from the complex (theoretical loss of 21.18%). In the third step, the decomposition temperature is in the range from 548.80 to 738.00 °C with a mass

dx.doi.org/10.1021/ie202891s | Ind. Eng. Chem. Res. 2012, 51, 4797−4803

loss of 20.07%, which roughly coincides with the value of 21.19% calculated for the loss of the other residual $(C_6H_4NO_2)^-$ from the complex.

The characteristic absorption bands of the IR spectra of the residue are similar to those of Sm_2O_3. Therefore, we concluded that the complex was decomposed into Sm_2O_3 completely (actual value, 33.72%; theoretical value, 32.36%). The high decomposition temperature of the complex suggests that the complex has good thermal stabilization. On the basis of experimental and calculated results, the thermal decomposition of $[Sm(C_6H_4NO_2)_2{\cdot}C_9H_6NO]$ can be postulated as follows:

$$2[Sm(C_6H_4NO_2)_2{\cdot}C_9H_6NO] \xrightarrow{\text{from 387.34 to 465.08°C}} [Sm(C_6H_4NO_2)_2]_2O \xrightarrow{\text{from 465.08 to 548.80°C}} 2[Sm(C_6H_4NO_2)O] \xrightarrow{\text{from 548.80 to 738.00°C}} Sm_2O_3$$

4.3. UV Spectra of the Complex. In the present work, we determined the UV spectra of the synthetic complex $[Sm(C_6H_4NO_2)_2{\cdot}C_9H_6NO]$ and the free ligands $C_6H_5NO_2$ and C_9H_7NO in the mixed solvent (V_{DMSO}/V_{EtOH} = 1:9). As shown in Figure 3, $C_6H_5NO_2$ has a maximum absorption at 263 nm due to

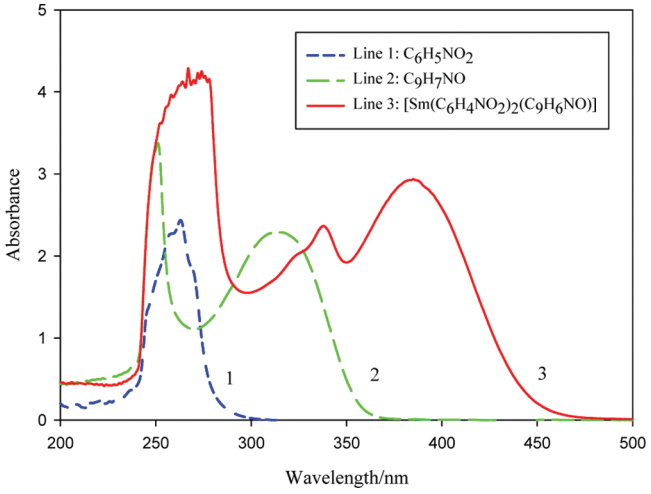

Figure 3. UV spectra of (1) nicotinic acid, $C_6H_5NO_2$; (2) 8-hydroxyquinoline, C_9H_7NO; and (3) the coordination complex $[Sm(C_6H_4NO_2)_2{\cdot}C_9H_6NO]$.

the π-to-π^* transition of the carboxyl and aromatic heterocycles. Free C_9H_7NO has a sharp and strong absorption peak at 246 nm ascribed to the absorption spectrum of the π-to-π^* transition of the condensed nucleus. In addition, there is a weaker broad peak at 316 nm, which belongs to the absorption spectrum of the n-to-π^* transition of the phenolic hydroxyl oxygen and cyclobenzene.

There are obvious differences between the UV spectra of the synthetic complex and those of the free ligands. The absorption band of the synthetic complex is significantly stronger and broader than that of every free ligand and it completely covers the absorption bands of the two free ligands. Moreover, the absorption band of the synthetic complex has an obvious red shift. As the number of aromatic rings of the complex and the conjugate degrees of the π bond increase, larger delocalization conjugate systems will form, all of which lead to the red shift and stronger absorption band of the π-to-π^* transition of the complex. In terms of quantum mechanics, if the value of ε is greater than 10^4 L·mol^{-1}·cm^{-1}, the transition can occur, whereas if it is less than 10^3 L·mol^{-1}·cm^{-1}, the chance of the transition is quite low. In the current case, the ε value of the complex falls in the range between 10^3 and 10^4 L·mol^{-1}·cm^{-1}, so the probability of the π-to-π^* transition of the complex is high. In fact, this strong absorption band ($\varepsilon \approx 4200$ L·mol^{-1}·cm^{-1}) appears at 240−290 nm in Figure 3. Additionally, a relatively weak absorption band appears at 350−430 nm, which is why the complex solution is yellow.

4.4. IR Spectra of the Complex. The main stretching frequencies of the IR spectra are tabulated in Table 2. As can be seen from Table 2 and Figure 4, there are obvious differences between the characteristic absorption bands of the complex and

Table 2. IR Data for the Ligands and the Complex $[SmL_2{\cdot}hq](s)$ (cm^{-1})

band	sample		
	$C_6H_5NO_2(s)$	$C_9H_7NO(s)$	$[SmL_2{\cdot}hq](s)$
ν_{O-H}	2200−2700	3136	
δ_{O-H}	951	1223	
$\nu_{C=O}$	1715		
$\nu_{as(COO^-)}$	1596		1594
$\nu_{s(COO^-)}$	1417		1407
$\nu_{C=C+C=N}$		1576	1571
ν_{Sm-O}			429

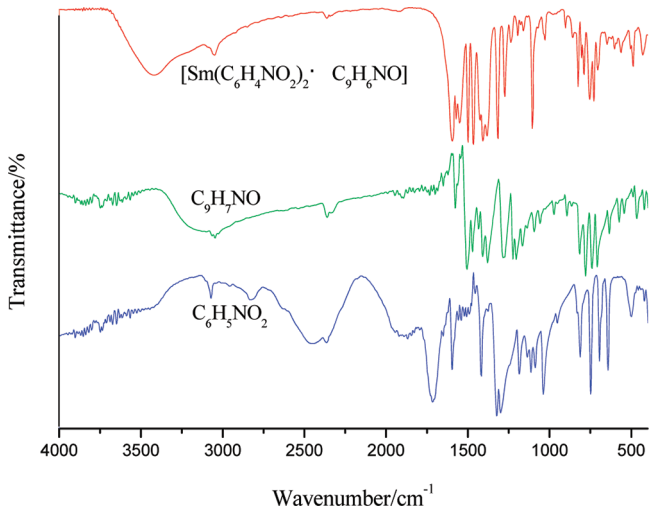

Figure 4. IR spectra of the free ligands and the synthetic complex.

the free ligands. After coordination, three characteristic absorption bands of the carboxylate group in the $C_6H_5NO_2$ ligand vanished, whereas the symmetric stretching vibration absorption band and asymmetric stretching vibration absorption band of COO^- remained. This fact confirmed that nicotinic acid, which removed the proton of carboxylic acid and existed in the form of an acidic group, was bidentate-coordinated with Sm^{3+}. For 8-hydroxyquinoline, the ν_{O-H} and δ_{O-H} bands vanished after the complex formed, which confirmed that C_9H_7NO was coordinated with Sm^{3+} after removal of the hydrogen of the hydroxyl group. In addition, the skeleton vibration peak of the quinoline ring shifted to a low wavenumber, decreasing by 5−7 cm^{-1}, indicating that the hydroxyl oxygen atom and

dx.doi.org/10.1021/ie202891s | Ind. Eng. Chem. Res. 2012, 51, 4797−4803

heterocyclic nitrogen atom of $C_9H_6NO^-$ were bidentate-coordinated with Sm^{3+} and formed a five-membered chelate ring, which increased the conjugation degree of the quinoline ring but decreased the bond strength of C═C and C═N. The single IR absorption band of the coordination complex appearing at 429 cm^{-1} was assigned to the stretching vibration of the Sm—O bond. Based on the above IR spectra and the data from elemental and thermogravimetric analyses, the chemical structure of the coordination complex is given in Figure 5.

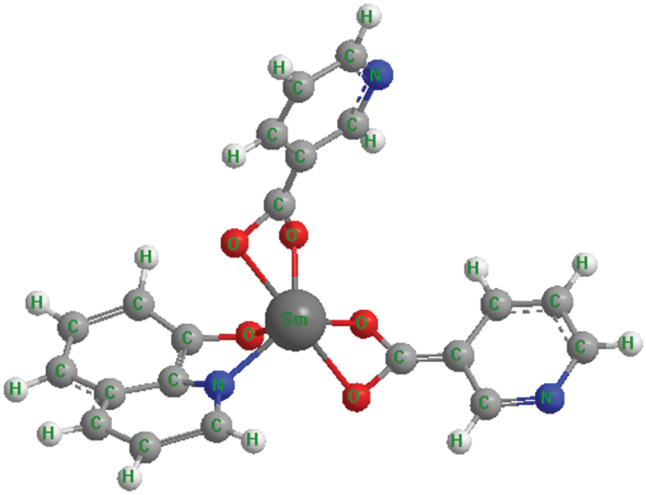

Figure 5. Chemical structure of the complex $[Sm(C_6H_4NO_2)_2{\cdot}C_9H_6NO]$.

4.5. X-ray Powder Diffraction of the Complex. To verify that the complex synthesized by our method is a pure compound, not a mechanical mixture of the reactants, we measured the X-ray powder diffraction pattern of the coordination complex. The details of the XRD analysis are shown in Figure 6.

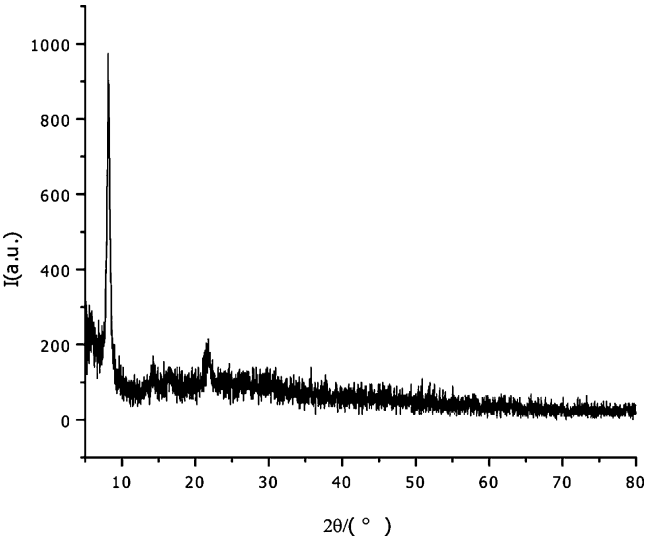

Figure 6. Powder XRD pattern of the coordination complex $[Sm(C_6H_4NO_2)_2{\cdot}C_9H_6NO]$.

As shown in Figure 6, the synthetic coordination complex was a single pure solid phase, not a multiphase mixture. This is because, theoretically speaking, the diffraction line of each phase should be contained in the XRD patterns if a substance measured contains two or more kinds of object phases. Further, by comparing the measured pattern with the JCPDS standard data card (no. 33-1954), it was demonstrated that the crystal type of $[Sm(C_6H_4NO_2)_2{\cdot}C_9H_6NO]$ was similar to that of $C_5H_{11}NO_2$. The cell parameters were a = 5.426 nm, b = 22.105 nm, and c = 5.277 nm.

4.6. Calorimetric Determination of the Enthalpy of Formation of the Complex. According to eq a

$$\begin{aligned}\Delta_r H_m^\Theta &= -\sum_B \nu_B \Delta_s H_{m,T,B}^\Theta \\ &= \Delta_s H_m^\Theta[C_9H_7NO(s), 298.15K] \\ &\quad + \Delta_s H_m^\Theta[2C_6H_5NO_2(s), 298.15K] \\ &\quad + \Delta_s H_m^\Theta[SmCl_3{\cdot}6H_2O(s), 298.15K] \\ &\quad - \Delta_s H_m^\Theta[Sm(C_6H_4NO_2)_2{\cdot}C_9H_6NO(s), 298.15K] \\ &\quad - \Delta_s H_m^\Theta[HCl(g), 298.15K] \\ &\quad - \Delta_s H_m^\Theta[\text{solution E}, 298.15K]\end{aligned}$$

The relevant dissolution enthalpies ($\Delta_s H_m^\Theta$) in this equation are given in Tables 1 and 3. Substituting the corresponding data into this equation gives

Table 3. Ancillary Thermodynamic Data

parameter	value ($kJ{\cdot}mol^{-1}$)	ref
$\Delta_s H_m^\Theta[HCl(g), 298.15\ K]$	−50.31	19
$\Delta_f H_m^\Theta[HCl(g), 298.15\ K]$	−92.31 ± 0.10	20
$\Delta_f H_m^\Theta[H_2O(1), 298.15\ K]$	−285.83 ± 0.04	20
$\Delta_f H_m^\Theta[C_6H_5NO_2(s), 298.15\ K]$	−344.81 ± 0.92	21
$\Delta_f H_m^\Theta[C_9H_7NO(s), 298.15\ K]$	−83.0 ± 1.5	22
$\Delta_f H_m^\Theta[SmCl_3{\cdot}6H_2O(s), 298.15\ K]$	−2870.2	23

$$\Delta_r H_m^\Theta = (167.49 \pm 0.39)kJ{\cdot}mol^{-1}$$

Also, through eq b, one can write

$$\begin{aligned}\Delta_r H_m^\Theta &= \sum_B \nu_B \Delta_f H_{m,T,B}^\Theta \\ &= \Delta_f H_m^\Theta[Sm(C_6H_4NO_2)_2{\cdot}C_9H_6NO(s), 298.15K] \\ &\quad + 3\Delta_f H_m^\Theta[HCl(g), 298.15K] \\ &\quad + 6\Delta_f H_m^\Theta[H_2O(l), 298.15K] \\ &\quad - 2\Delta_f H_m^\Theta[C_6H_5NO_2(s), 298.15K] \\ &\quad - \Delta_f H_m^\Theta[C_9H_7NO(s), 298.15K] \\ &\quad - \Delta_f H_m^\Theta[SmCl_3{\cdot}6H_2O(s), 298.15K]\end{aligned}$$

so that

$$\begin{aligned}&\Delta_f H_m^\Theta[Sm(C_6H_4NO_2)_2{\cdot}C_9H_6NO(s), 298.15K] \\ &= \Delta_r H_m^\Theta + 2\Delta_f H_m^\Theta[C_6H_5NO_2(s), 298.15K] \\ &\quad + \Delta_f H_m^\Theta[C_9H_7NO(s), 298.15K] \\ &\quad + \Delta_f H_m^\Theta[SmCl_3{\cdot}6H_2O(s), 298.15K] \\ &\quad - 3\Delta_f H_m^\Theta[HCl(g), 298.15K] \\ &\quad - 6\Delta_f H_m^\Theta[H_2O(l), 298.15K]\end{aligned}$$

According to the auxiliary thermodynamic data listed in Table 3 and the above calculated result $\Delta_r H_m^\Theta = (167.49 \pm 0.39)\ kJ{\cdot}mol^{-1}$,

dx.doi.org/10.1021/ie202891s | Ind. Eng. Chem. Res. 2012, 51, 4797−4803

the standard molar enthalpy of formation of the synthetic complex can be obtained as

$$\Delta_f H_m^{\Theta}[Sm(C_6H_4NO_2)_2\cdot C_9H_6NO(s), 298.15K] = -(1483.4 \pm 2.4)kJ\cdot mol^{-1}$$

4.7. Experimental Discussion. As shown by the results calculated in the preceding section, the standard molar enthalpy change of the coordination reaction, $\Delta_r H_m^{\Theta} = (167.49 \pm 0.39)$ kJ·mol^{-1}, is a large positive value. This indicates that the reactants cannot spontaneously mutually react in the solid state. Because the thermal effect of the solid-state coordination reaction is difficult to determine, some other methods should be employed to measure it. In this work, we designed a convincing thermochemical cycle based on Hess's law and deduced the standard molar enthalpy of formation from the dissolution enthalpies that were measured with an advanced solution−reaction isoperibol microcalorimeter when the samples were dissolved in the optimal calorimetric solvent.

The calculated standard molar enthalpy of formation of the synthetic rare earth coordination complex $[Sm(C_6H_4NO_2)_2\cdot C_9H_6NO]$ is comparedwith those of similar rare earth coordination complexes, such as $[La(C_6H_4NO_2)_2\cdot C_9H_6NO]\cdot 2H_2O$ and $[Ce(C_6H_4NO_2)_2\cdot C_9H_6NO]\cdot 2H_2O$ reported by Xiao et al.,[24] in Figure 7.

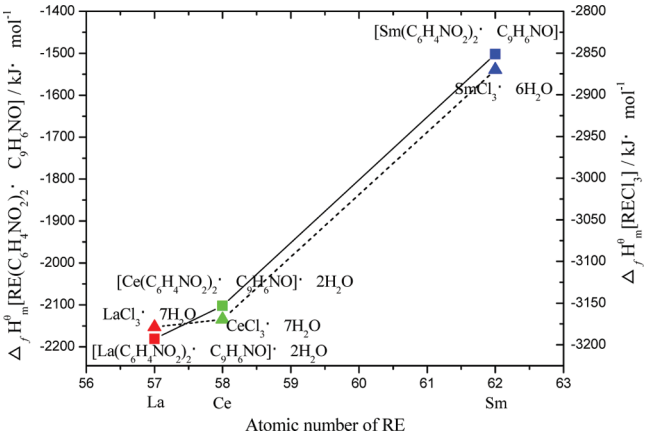

Figure 7. Plot of the standard molar enthalpies of formation, $\Delta_f H_m^{\Theta}[RE(C_6H_4NO_2)_2\cdot C_9H_6NO(s)]$ and $\Delta_f H_m^{\Theta}[RECl_3(s)]$, of the synthetic rare earth coordination complexes $[RE(C_6H_4NO_2)_2\cdot C_9H_6NO]$ (s) (■) and the corresponding rare earth chlorides $[RECl_3](s)$ (▲) as a function of the atomic number of rare earth (RE) element.

It can be seen from Figure 7 that the standard molar enthalpies of formation of the synthetic rare earth coordination complexes, $\Delta_f H_m^{\Theta}[RE(C_6H_4NO_2)_2\cdot C_9H_6NO(s)]$, increase with increasing atomic number of the rare earth (RE) element, but the relationship is not linear. The probable reason for this type of phenomenon is that the standard molar enthalpies of formation of a series of similar rare earth coordination complexes depend not only on the atomic number of the center ions but also the crystal structures and various bonding forces of the complexes. The relationship between the standard molar enthalpies of formation of the corresponding rare earth chlorides, $[RECl_3](s)$, and the atomic numbers of the rare earth (RE) elements is also presented in Figure 7. It was found that the standard molar enthalpies of formation of the corresponding rare earth chlorides $[RECl_3](s)$ have the same change tendency as those of the synthetic rare earth coordination complexes as a function of the atomic number of the rare earth (RE) elements contained therein.

5. CONCLUSIONS

A novel rare earth coordination complex was synthesized using three raw materials: $SmCl_3\cdot 6H_2O$, C_9H_7NO, and $C_6H_5NO_2$. Its composition and structure were characterized by elemental analysis, molar conductance, thermogravimetric analysis (TG−DTG), UV spectroscopy, IR spectroscopy, and X-ray powder diffraction. The analytical results showed that the composition of the complex was $[Sm(C_6H_4NO_2)_2\cdot C_9H_6NO]$ and that its purity was more than 99.0%; the crystal type of $[Sm(C_6H_4NO_2)_2\cdot C_9H_6NO]$ was similar to that of $C_5H_{11}NO_2$, and the cell parameters were a = 5.426 nm, b = 22.105 nm, and c = 5.277 nm. Particularly, an advanced solution−reaction isoperibol microcalorimeter was employed to determine the standard molar enthalpy of formation of the synthetic coordination complex. According to Hess's law and thermodynamic principles, a reasonable thermochemical cycle was designed. At 298.15 K, the dissolution enthalpies were measured when the relevant substances were dissolved in the optimal calorimetric solvent. The standard molar enthalpy change of the reaction was determined from the experimental data to be $\Delta_r H_m^{\Theta} = (167.49 \pm 0.39)$ kJ·mol^{-1}. From this molar enthalpy change of the coordination reaction and other auxiliary thermodynamic quantities, the standard molar enthalpy of formation of the synthetic coordination complex $[Sm(C_6H_4NO_2)_2\cdot C_9H_6NO](s)$ was derived to be $\Delta_f H_m^{\Theta}[Sm(C_6H_4NO_2)_2\cdot C_9H_6NO(s), 298.15\ K] = -(1483.4 \pm 2.4)$ kJ·mol^{-1}.

The present work demonstrated that solution−reaction microcalorimetry is a very useful tool for thermodynamic research, as it is capable of providing accurate thermodynamic quantities of many important substances in industrial and scientific research. This work provides sufficient thermal and thermodynamic data for a novel rare earth coordination complex that this information will enrich and develop the fundamental thermodynamic database of rare earth coordination complexes and consequently could have theoretical instructive significance and application values for the research and development of rare earth coordination complexes.

■ ASSOCIATED CONTENT

Ⓢ Supporting Information

Purities, sources, and purification methods of the chemicals and reagents used in this work, diagram of the microcalorimeter, and IR spectra of the coordination complex and the free ligands. This material is available free of charge via the Internet at http://pubs.acs.org.

■ AUTHOR INFORMATION

Corresponding Author

*Tel.: + (86) 735 2653129. Fax: + (86) 735 2653129. E-mail: 54xsx@163.com.

Notes

The authors declare no competing financial interest.

■ ACKNOWLEDGMENTS

This research was financially supported by the National Natural Science Foundation of China (No. 20973145), the Scientific Research Foundation of Hunan Provincial Education Department (No. 11C1171), and the Scientific Research Foundation of Xiangnan University (No. 2010Y061). The authors thank Xiao-Li Yin (State Key Laboratory of Chemo/Biosensing &

Chemometrics, Hunan University, Changsha, China) for her help in revising our manuscript.

REFERENCES

(1) Yang, L; Tao, D.; Yang, X.; Li, Y.; Guo, Y. Synthesis, Characterization, and Antibacterial Activities of Some Rare Earth Metal Complexes of Pipemidic acid. *Chem. Pharm. Bull.* **2003**, *51*, 494−502.
(2) Zhou, J.; Wang, L. F.; Wang, J. Y.; Tang, N. Synthesis, Characterization, Antioxidative and Antitumor Activities of Solid Quercetin Rare Earth(III) Complexes. *J. Inorg. Biochem.* **2001**, *83*, 41−49.
(3) Di, Y. Y.; Kong, Y. X.; Zhang, S.; Yang, W. W.; Wu, E. S.; Shi, Q.; Tan, Z. C. Synthesis, Characterization and Thermochemistry of the Hydrated Barium Nicotinate. *Acta Phys. Chim. Sin.* **2008**, *24*, 1884−1890.
(4) Darby, C. M.; Nathan, C. F. Killing of Non-Replicating Mycobacterium Tuberculosis by 8-Hydroxyquinoline. *J. Antimicrob. Chemother.* **2010**, *65*, 1424−1427.
(5) Sashidhara, K. V.; Kumar, A.; Bhatia, G.; Khan, M. M.; Khanna, A. K.; Saxena, J. K. Antidyslipidemic and Antioxidative Activities of 8-Hydroxyquinoline Derived Novel Keto-Enamine Schiffs Bases. *Eur. J. Med. Chem.* **2009**, *44*, 1813−1818.
(6) Liu, Y. J.; Zhao, Y.; Zhai, X.; Feng, X.; Wang, J.; Gong, P. Synthesis and Anti-Hepatitis B Virus Evaluation of Novel Ethyl 6-Hydroxyquinoline-3-carboxylates in Vitro. *Bioorg. Med. Chem.* **2008**, *16*, 6522−6527.
(7) Li, X.; Li, Q. G.; Zhang, H.; Hu, J. L.; Yao, F. H.; Yang, D. J.; Xiao, S. X.; Ye, L. J.; Huang, Y.; Guo, D. C. Synthesis and Bioactive Studies of Complex 8-Hydroxyquinolinato-Bis-(Salicylato) Yttrium (III). *Biol. Trace Elem. Res.*, published online Dec. 13, 2011, http://dx.doi.org/10.1007/s12011-011-9297-1.
(8) Yang, D. J.; Li, X.; Hu, J. L.; Yao, F. H.; Xiao, S. X.; Yang, L. L.; Xiang, Y. L.; Li, Q. G. Synthesis, Standard Molar Enthalpy of Formation and Microcalorimetric Study on the Anti-*S. pombe* Effect for the Complex Manganese Nicotinate $[Mn(C_6H_4NO_2)_2]\cdot 2H_2O$. *Acta Chim. Sin.* **2010**, *68*, 2373−2380.
(9) Zhang, J. J.; Wang, R. F.; Liu, H. M. Kinetics of the Complex of Terbium *o*-Methylbenzoate with 1,10-Phenanthroline Synthesis, Decomposition Mechanism. *J. Therm. Anal. Calorim.* **2001**, *66*, 431−437.
(10) Zhang, J. J.; Zhang, H. Y.; Xu, S. L.; Ren, N.; Wang, R. F.; Wang, S. P. Synthesis and Crystal Structure of the Complex $[Sm(p\text{-}MOBA)_3bipy]_2\cdot 2C_2H_5OH$. *Russ. J. Inorg. Chem.* **2010**, *55*, 739−745.
(11) Li, Q. G.; Zhang, H.; Li, X.; Wang, B.; Hu, J. L.; Yao., F. H.; Yang, D. J.; Xiao, S. X.; Ye, L. J. Synthesis of Thioproline Salicylic Acid Samarium Complex and Microcalorimetric Study on Effects of the Complex on the Growth Metabolism of *S. pombe* Cells. *Chin. J. Chem.* **2011**, *29*, 2285−2292.
(12) Li, Q. G.; Yang, D. J.; Li, X.; Ye, L. J.; Wei, D. L.; Xiao, S. X. Thermokinetic Studies of Action of Complexes $RE(Hsal)_2\cdot(tch)\cdot 2H_2O$ on Growth Metabolism of *Escherichia coli*. *Acta Chim. Sin.* **2008**, *66*, 2686−2692.
(13) Suga, H. Perspectives of Low Temperature Calorimetry. *Thermochim. Acta* **2000**, *355*, 69−82.
(14) Ferguson, H. F.; Frurip, D. J.; Pastor, A. J.; Apeerey, L. M.; Whiting, L. F. A Review of Analytical Applications of Calorimetry. *Thermochim. Acta* **2000**, *363*, 1−21.
(15) Xiao, S. X.; Gu, H. W.; Zhang, J. J.; Xiao, H.; Ding, J.; Lu, X. Synthesis, Characterization, and Thermochemical Study on a Ternary Complex $[Sm(m\text{-}MOBA)_3phen]_2$. *Int. J. Thermophys.* **2012**, *33*, 289−299.
(16) Ribeiro da Silva, M. A. V.; Ribeiro da Silva, M. D. M. C.; da Silva, L. C. M.; Dietze, F.; Hoyer, E. Thermochemical Studies of Two Copper(II) Complexes with *N*-Benzoyl-*N*′,*N*′-dialkylurea Derivatives. *Thermochim. Acta* **2001**, *378*, 45−50.
(17) Yu, H. G.; Liu, Y.; Tan, Z. C.; Dong, J. X.; Zou, T. J.; Huang, X. M.; Qu, S. S. A Solution−Reaction Isoperibol Calorimeter and Standard Molar Enthalpies of Formation of $Ln(hq)_2Ac$ (Ln = La, Pr). *Thermochim. Acta* **2003**, *401*, 217−224.
(18) Rychly, R.; Pekarek, V. The Use of Potassium Chloride and Tris(hydroxymethyl) Aminomethane as Standard Substances for Solution Calorimetry. *J. Chem. Thermodyn.* **1977**, *9*, 391−396.
(19) Xiao, S. X.; Zhang, J. J.; Li, X.; Ye, L. J.; Gu, H. W.; Ren, N. Synthesis and Thermochemical Properties of the Ternary Complex $[Sm(m\text{-}NBA)_3phen]_2\cdot 2H_2O$. *J. Chem. Eng. Data* **2010**, *55*, 1688−1692.
(20) Cox, J. D.; Wagman, D. D.; Medvedev, V. A. *CODATA Key Values for Thermodynamics*; Hemisphere Publishing Corp.: New York, 1984; p 1.
(21) Sato-Toshima, T.; Kamagughi, A.; Nishiyama, K.; Sakiyama, M.; Seki, S. Enthalpies of Combustion of Organic Compounds. IV. Acetaneilide and Nicotinic Acid. *Bull. Chem. Soc. Jpn.* **1983**, *56*, 51−54.
(22) Ribeiro da Silva, M. A. V.; Monte, M. J. S.; Matos, M. A. R. Enthalpies of Combustion, Vapour Pressures, and Enthalpies of Sublimation of 8-Hydroxyquinoline, 5-Nitro-8-hydroxyquinoline, and 2-Methyl-8-hydroxyquinoline. *J. Chem. Thermodyn.* **1989**, *21*, 159−166.
(23) Weast, R. C. *CRC Handbook of Chemistry and Physics*, 69th ed.; CRC Press Inc.: Boca Raton, FL, 1988/1989; p D-121.
(24) Xiao, S. X.; Gu, H. W.; Liu, Y. T.; Luo, W.; Xiao, F. B.; Li, Q. G. Preparation and Thermochemical Properties of Ternary Complexes of Rare Earth Chlorides with Nicotinic Acid and 8-Hydroxylquinoline. *J. Chem. Eng. Data* **2012**, *57*, 269−273.